Journal of Alloys and Compounds 488 (2009) 250–253

Contents lists available at ScienceDirect

Journal of Alloys and Compounds

journal homepage: www.elsevier.com/locate/jallcom

The luminescence characteristics of ZnS_xSe_{1-x} phosphor powder

T.P. Tang*, W.L. Wang, S.F. Wang

Department of Materials and Mineral Resources Engineering, National Taipei University of Technology, Taipei, Taiwan

ARTICLE INFO

Article history:
Received 30 March 2009
Received in revised form 19 August 2009
Accepted 22 August 2009
Available online 27 August 2009

Keywords:
ZnS_xSe_{1-x}
Phosphor
Luminescence

ABSTRACT

In this study, the effects of processing on the phosphor characteristics of ZnS_xSe_{1-x} powder were performed. The ZnS used in this experiment is a green light powder, and the ZnSe is a red light powder. Phosphor powder with green light to red light emission can be obtained using mixtures of ZnS and ZnSe with different ratios. Results indicated that prolong the soaking time of the mixtures at 1000–1100 °C, a better luminescent intensity is obtained. It is due to the oxygen enters into ZnSSe lattice, which results in the distortion of the crystal lattice and the formation of the crystal defects.

1. Introduction

Electro-luminescent Display (ELD) have some advantages [1–3] compared with Liquid Crystal Display (LCD), such as low cost, wide operate temperature (−40 °C to 80 °C), high contrast (170:1), wide visual angle (±80 °C), high brightness (100 cd/m^2), thin layer (2 mm), short response time (<1 ms), and light in weight. The key parameters for a good phosphor powder used in practical ELD applications include accurate colors, uniform brightness, and long life [4]. Common ELD phosphor powders involve ZnS, ZnSe, $BaTiO_3$, and TiO_2 [5–8]. In the literature, most ZnS–ZnSe powders reported were prepared by PVD or MOPVD methods [9–12]. In this paper, ZnS–ZnSe powders were prepared using solid state reaction method. The effects of the processing on the structure and PL property of ZnS_xSe_{1-x} powders were evaluated.

2. Experimental procedure

ZnS_xSe_{1-x} phosphors were prepared using solid state process form commercial available ZnS and ZnSe powders. ZnS_xSe_{1-x} powders were synthesized through the reaction of ZnS + ZnSe ⇔ ZnSSe. ZnS and ZnSe powders were mixed in DI water with rotating magnet, and then dried in 100 °C water bath. The dry powders were again dispersed in an alcohol solution and then dried in an oven at 105 °C, to prevent any agglomeration. The dispersed powders were put in a platinum crucible, and then loaded in a tubular furnace. The powders were fired at temperatures between 800 °C and 1100 °C in an inert atmosphere for 1 h. After firing, the powders were taken out from the furnace and quenched on a stainless steel plate in air. After 5 min, the cooled powders were ground using mortar and pestle. The typical process flow chart is shown in Fig. 1. The emission spectra and the excitation spectra were measured by a spectrofluorophotometer (Shimadzu RF-5301), which is equipped with the standard lamp. The excitation spectra can be obtained by scanning wavelength from 220 nm to 450 nm, emissive at 650 nm. The emission wavelength was scanned from 500 nm to 750 nm, excited at 405 nm. X-ray diffraction (XRD) was used to identify the structures of the products using a Rigaku D/Max B with Cu Kα1 radiation at 40 kV. SEM micrographs of the powders were characterized using a field emission scanning electron microscopy (Hitachi Company launches S-4700).

3. Results and discussion

The XRD diagram of commercial ZnS fired at 1100 °C for 30 min is shown in Fig. 2. It indicates that some ZnO phase formed when fired in nitrogen atmosphere. Crystal structure of ZnS contains a major cubic phase, minor hexagonal phase and ZnO phase. The calculated lattice constant for the cubic phase is 3.977 Å, which is smaller than that of typical cubic ZnS (4.009 Å). Nitrogen atoms were incorporated into the ZnS lattice during firing and resulted in the construction of the unit cell. SEM micrograph of commercial ZnS powder is shown in Fig. 3. The powder has an average particle size of 2.8 μm and an irregular morphology, which indicates the small growth of the powders.

The influence of firing temperature on PL property of pure ZnSe powder is shown in Fig. 4. The luminescence intensity is increased dramatically when the firing temperature is increased from 800 °C to 1000 °C. As the firing temperature increases, the crystallization becomes faster and little oxidation occurred, which enhanced the luminescence intensity. The more oxygen entered the ZnSe lattice, the larger lattice distortion was observed, that increases emitting intensity. The PL emitting intensities of ZnSe fired at 1000 °C and 1100 °C are near the same, because they have a similar level of crystallization and ZnO formation. The SEM diagram of pure ZnSe powder is shown in Fig. 5. The powder has an average particle size of ≈1.7 μm and a round morphology. Only little particle growth was observed. The influence of the soaking time at 1100 °C on the PL property of pure ZnSe is shown in Fig. 6. For the soaking time

* Corresponding author.
E-mail address: tptang@ntut.edu.tw (T.P. Tang).

0925-8388/$ – see front matter © 2009 Elsevier B.V. All rights reserved.
doi:10.1016/j.jallcom.2009.08.098

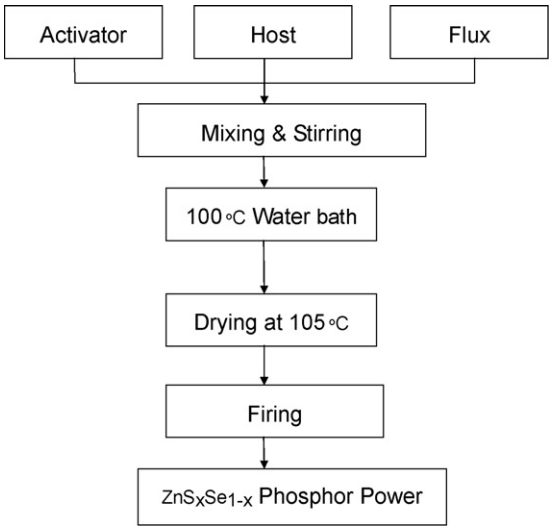

Fig. 1. Flow chart for the preparation of the ZnS_xSe_{1-x} phosphor powders.

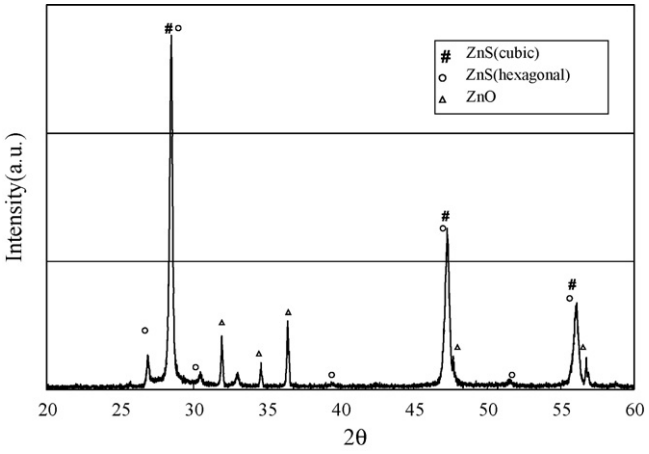

Fig. 2. The XRD patterns of commercial ZnS fired at 1100 °C for 30 min.

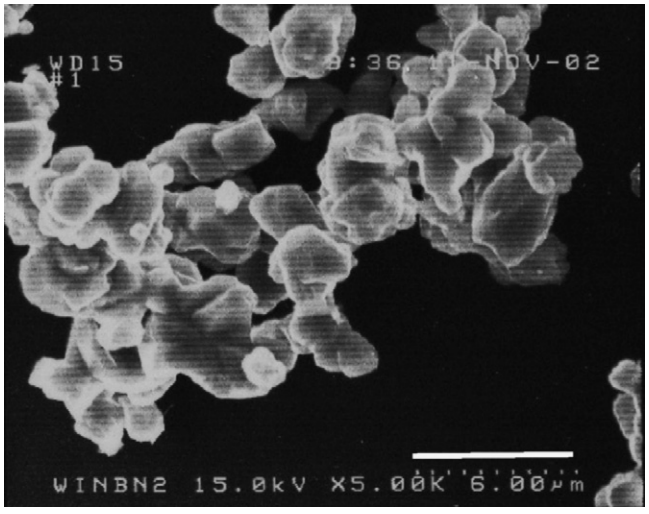

Fig. 3. The SEM diagram of commercial ZnS powder (5000×).

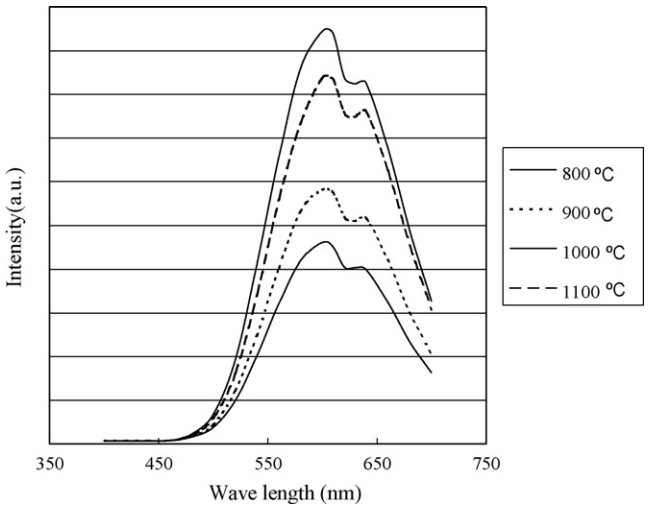

Fig. 4. The influence of the firing temperature on the PL property of the pure ZnSe powder (exciting at 379 nm).

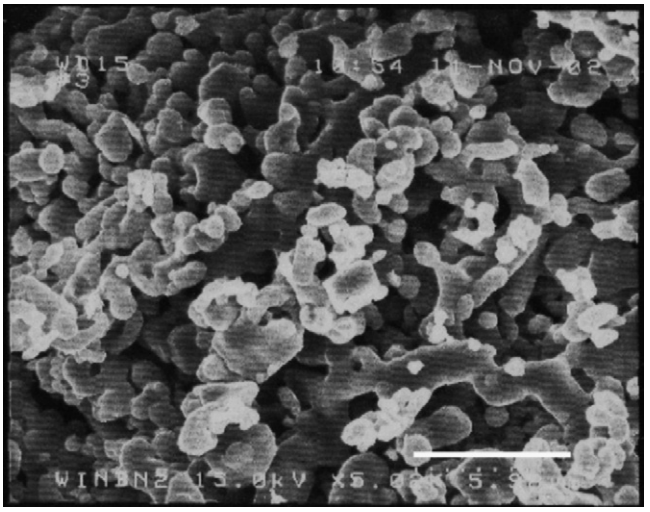

Fig. 5. The SEM diagram of the pure ZnSe powder (5000×).

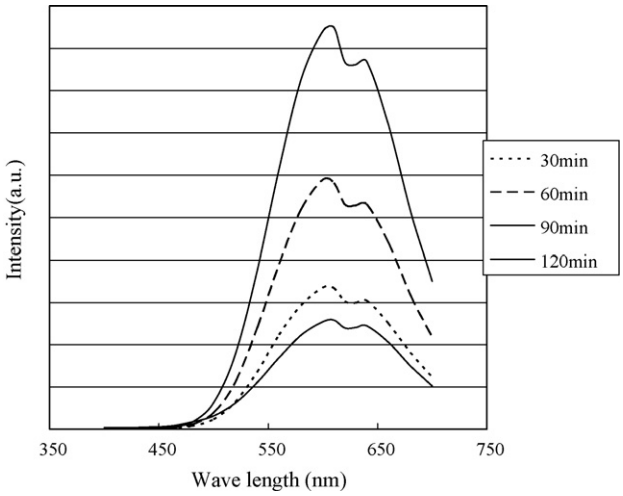

Fig. 6. The influence of the soaking time at 1100 °C on the PL property of the pure ZnSe (exciting at 381 nm).

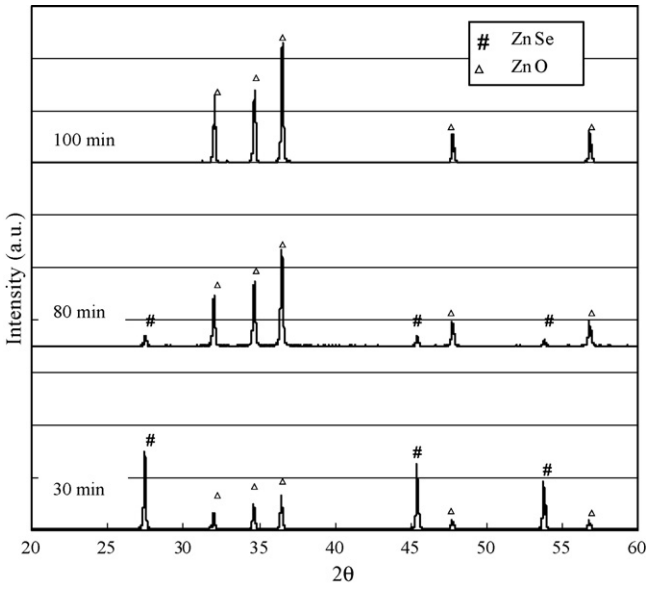

Fig. 7. The XRD patterns of the pure ZnSe powder fired at 1000 °C for different soaking times.

of 30 min and 60 min, two phase structure including ZnSe and ZnO is observed, which is due to the fact that oxygen atoms enter the ZnSe lattice, as shown in XRD results (Fig. 7). It causes the lattice distortion and thus increases the emitting intensity. As the soaking times exceed 90 min, the ZnSe phase disappears completely, and only ZnO exists. The lattice distortion becomes less and the PL intensity decreases rapidly. The remained ZnO phase makes the PL intensity weak; however, the color of the emission is not altered.

The influence of the mole ratios of S/Se on the exciting and emitting wavelength of ZnS_xSe_{1-x} is shown in Table 1. It indicates that commercial ZnS powder emits a green light, and pure ZnSe powder generates a red light. For a mixture of commercial ZnS and ZnSe, the color of emission varies from red light to orange light, absinth light and finally green light, by increasing the commercial ZnS content. The exciting and emitting wavelengths are declined from 465 nm to 340 nm and from 644 nm to 505 nm, respectively, by increasing commercial ZnS content. The lattice constant and cell volume of cubic ZnSSe calculated from XRD results are 4.118 Å and 69.81 $Å^3$, respectively. They are larger than those of typical ZnSSe (4.082 Å and 68.08 $Å^3$), due to the substitution of O atoms. The lattice constants and cell volume of ZnO are $a = 7.642$ Å and $c = 3.484$ Å and 524.12 $Å^3$, respectively, which are smaller than those of hexagonal ZnO ($a = 7.656$ Å and $c = 3.484$ Å and 530.56 $Å^3$), due to the substitution of Se atoms.

The influence of soaking time (1100 °C) on PL property of $ZnS_{0.69}Se_{0.31}$ is shown in Fig. 8. Similar to that observed in ZnSe powder, more oxygen enters into ZnS_xSe_{1-x} was substituted by O, it makes the atomic ratio of Se in ZnS_xSe_{1-x} increased. The right side of emitting spectrum is thus raised.

Table 1
The influence of the mole ratios of S/Se on the exciting and emitting wavelength of ZnS_xSe_{1-x}.

ZnS (mol%)	Exciting wavelength (nm)	Emitting wavelength (nm)	Light color
0	465	644	Red
27	406	591	Orange
50	383	573	Green–yellow
69	372	561	Absinth
85	355	538	Yellow–green
100	340	505	Green

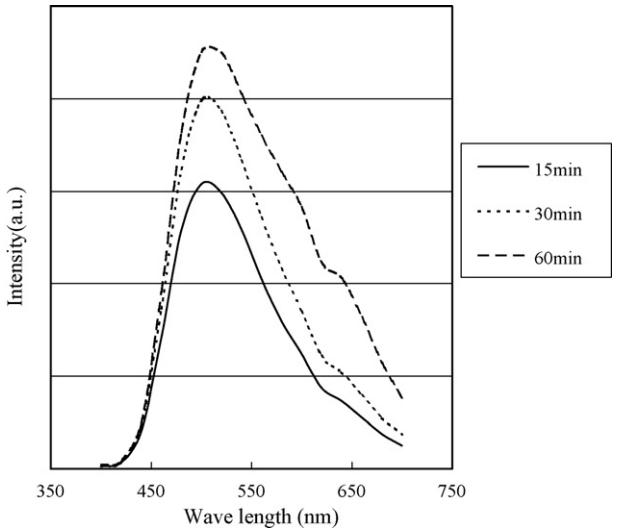

Fig. 8. The influence of the firing time at 1100 °C on the PL property of the $ZnS_{0.69}Se_{0.31}$ powder (exciting at 382 nm).

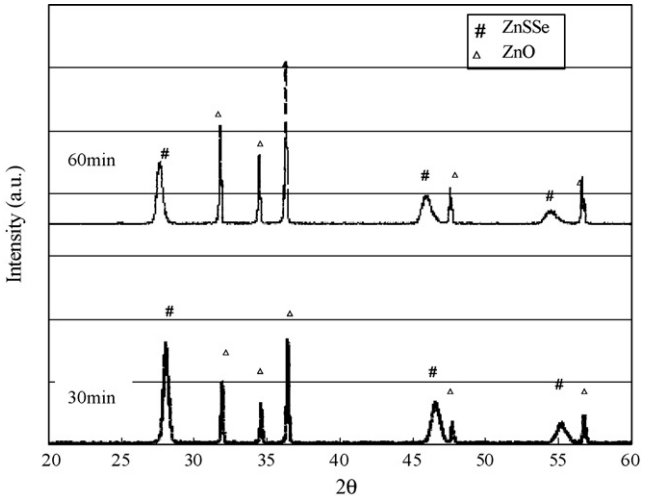

Fig. 9. The XRD patterns of $ZnS_{0.69}Se_{0.31}$ powders prepared using different soaking time at 1100 °C.

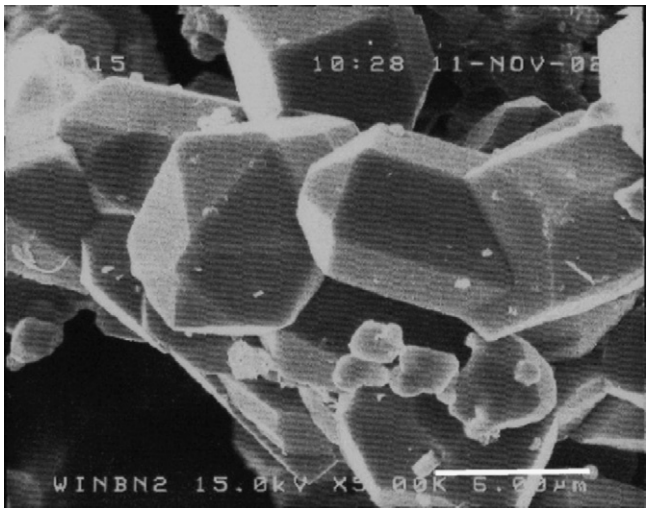

Fig. 10. The SEM diagram of the $ZnS_{0.69}Se_{0.31}$ powder (5000×).

XRD results of $ZnS_{0.69}Se_{0.31}$ fired at 1100 °C for 30 min and 60 min are shown in Fig. 9. It shows that there are two phases coexisted, including ZnO and ZnSSe. Existence of these two phases induces the lattice distortion, thus increases the luminescence intensity. SEM micrograph of $ZnS_{0.69}Se_{0.31}$ is shown in Fig. 10. It indicates that ZnS_xSe_{1-x} powder has an average particle diameter of ≈4.5 μm with cylinder morphology, which is larger than those of individual commercial ZnS and ZnSe powders. This manifests the particle growth during the formation of ZnS_xSe_{1-x} solution, from ZnS and ZnSe.

4. Conclusions

For pure ZnSe system, the intensity of PL emitting increases with the firing temperature. However, it levels off as the firing temperature exceeds 1000 °C. With the increasing of soaking time, oxygen atoms enter into ZnS_xSe_{1-x} or ZnSe lattice, which leads to the lattice distortion, and thus enhances the luminescence intensity. By controlling the ratio of ZnS and ZnSe phases, the emitting wavelength varies from 500 nm to 640 nm. The color of emitted light changes from green, to absinth, orange, and red. By controlling the firing conditions such as temperature and soaking time, the PL intensity is altered. For example, in $ZnS_{0.69}Se_{0.31}$ system, when soaking time become longer, the emitting intensity is enhanced.

References

[1] Yoshimasa A. Ono, Electroluminescent Displays (Information Display, Vol.1), World Scientific Publishing Company, 1995, 1-8.
[2] A.H. Kitai, Solid State Luminescence, Chapman & Hall, 1993, pp. 166–204.
[3] Alexey N. Krasnov, Displays 24 (2003) 73–79.
[4] Markku Leskelä, J. Alloys Compd. 275/277 (1998) 702–708.
[5] T. Toyama, K. Yoshimura, M. Fujii, H. Haze, H. Okamoto, Appl. Surf. Sci. 244 (2005) 524–527.
[6] T.P. Tang, Ceramics Int. 33 (2007) 1251–1254.
[7] A.N. Krasnov, J.P. Bender, W.Y. Kim, Thin Solid Films 467 (2004) 247–252.
[8] Y.J. Lin, Y.K. Su, M. Yokoyama, Appl. Surf. Sci. 65/66 (1993) 461–464.
[9] Udo W. Pohl, et al., J. Crystal Growth 214/215 (2000) 717–721.
[10] T.P. Srukova, et al., J. Crystal Growth 214/215 (2000) 576–580.
[11] S. Armstrong, P.K. Datta, R.W. Miles, Thin Solid Films 403/404 (2002) 126–129.
[12] K. Swiatek, M. Godlewski, V.Y. Ivanov, J. Alloys Compd. 371 (2004) 195–197.